**Oncogene (1998) 16,** 2051–2063

http://www.stockton-press.co.uk/onc

# Cytosol is the prime compartment of hepatitis B virus X protein where it colocalizes with the proteasome

Hüseyin Sirma[1], Robert Weil[2], Olivier Rosmorduc[1], Stephan Urban[3], Alain Israël[2], Dina Kremsdorf[1] and Christian Bréchot[1]

*[1]INSERM U370, Carcinogénèse Hépatique et Virologie Moléculaire, Necker Institut, 156 rue de Vaugirard, 75015 Paris; [2]Unite de Biologie Moléculaire de l'Expression Génique, URA 1149, Institut Pasteur, 25 rue du Dr. Roux, 75724 Paris Cedex 15; [3]Department of Virus Research, Max-Planck-Institute for Biochemistry, Am Klopferspitz 18a, D-82152 Martinsried, Germany*

**The hepatitis B virus X protein plays an important role in the regulation of viral genome expression and has also been implicated in the development of liver cancer associated with chronic viral infection. Several effects have been attributed to X but their biological relevance remains elusive. One of the confusing issues has been so far the uncertainty concerning its cellular location. To gain insight into the mechanism(s) how X exerts its effects, we have analysed its subcellular distribution and its dependency on the cell cycle. We used two complementary approaches namely, immunolocalization using a cell line stably expressing X, and characterization of the dynamics of X location in living cells by means of the reporter gene GFP. Our data clearly define the cytosol as the prime location of X, irrespectively of the cell cycle and show in addition the close attachment of a fraction of X to the nuclear membrane. However, X does not associate with any cytoplasmic vesicles and organelles so far tested. In contrast, our study provides strong evidence for the codistribution of X with the cytosolic fraction of proteasomes. In pulse-chase experiments, X decayed with a half-life of less than 30 min and proteasome-inhibitors did not modify its turnover, suggesting that X colocalization with the proteasome does not simply point to its degradation pathway. The proteolytic processing of the p105 precursor of the p50 subunit of the NF-κB transcription factor, which has been shown to be proteasome-dependent, is markedly slow down in the presence of X. These findings suggest that X modulates the processing rate of p105 by acting presumably at the level of the proteasome. Thus, targeting of proteasomes by X might be one of the pathways employed by this viral protein to subvert cellular functions.**

**Keywords:** hepatitis B virus; X protein; proteasomes; NF-κB

## Introduction

The X-ORF is highly conserved among all mammalian hepadnaviruses, suggesting the biological importance of the X-protein in the viral life cycle (Kodama *et al*., 1985). X is expressed during natural infections in mammals and antibodies to X have been detected in the sera of patients with both acute and chronic hepatitis (Persing *et al*., 1986; Hess *et al*., 1988; Levrero *et al*., 1991). Chronic infection by HBV is strongly associated with the development of liver cancer (Beasley *et al*., 1981) and several lines of evidence emphasize the involvement of X in this process (for a review, see Hildt *et al*., 1996). Furthermore, X is required for viral infectivity *in vivo* (Chen *et al*., 1993; Zoulim *et al*., 1994) and enhances viral protein synthesis and pregenomic transcription *in vitro* (Colgrove *et al*., 1989; Spandau and Lee, 1988). Thus, X might regulate the expression of certain viral and cellular genes important for the creation of an environment suitable for viral propagation.

It is generally thought that the transcriptional activity of X is essential for its effects and several studies point to different mechanisms (for a review, see Yen, 1996 and Hildt *et al*., 1996). The fact that X by itself does not bind to dsDNA (Avantaggiati *et al*., 1993; Siddiqui *et al*., 1987) and that genes stimulated by X lack any obvious consensus sequences suggest interaction of X with cellular proteins and/or components of the signal transduction pathways. Indeed, X interacts and modifies *in vitro* the DNA-binding affinity of transcription factors, namely CREB/ATF (Maguire *et al*., 1991; Williams and Andrisani, 1995), TATA box binding protein (TBP) (Qadri *et al*., 1995) and the RBP5 subunit of RNA polymerase II (Cheong *et al*., 1995). Regarding the signal transduction pathways, X activates those associated with protein kinase C (PKC) (Kekulé *et al*., 1993), or Ras/Raf mitogen-activated protein (MAP) kinase (Seto *et al*., 1990; Benn and Schneider, 1994). X also stimulates NF-κB-dependent transcription (Chirillo *et al*., 1996; Su and Schneider, 1996). This has potentially major biological implications, since NF-κB regulates a large number of genes involved in the immune response and in inflammatory processes (for a review, see Baldwin *et al*., 1996). As well as being activated by a large variety of stimuli including lipopolysaccharide, TNF-α, IL1β and double stranded RNA, NF-κB is also activated by viral proteins with an oncogenic potential such as human T-cell leukemia virus type 1 (HTLV-1) Tax and human immunodeficiency virus-type 1 (HIV-1) Tat (for a review, see Baldwin, 1996). The function of NF-κB is strictly regulated by its subcellular localization: most NF-κB proteins are in an inactive form in the cytoplasm, bound to specific inhibitory proteins called IκB. p105 and p100, the precursors of the NF-κB subunits p50 and p52, respectively, also behave as IκBs. They associate with and retain various NF-κB subunits in the cytoplasm. These precursors are

Correspondence: C Bréchot
Received 18 August 1997; revised 20 November 1997; accepted 21 November 1997

processed by a proteasome-dependent mechanism leading to mature DNA binding subunits, which are originally localized in their N-terminal region while the C-terminal region is degraded by the ubiquitin-proteasome pathway (Palombella *et al*., 1994).

Despite extensive progress in recent years in understanding the cellular effects of X, studies attributing biological significance to any of these effects are lacking. The variability of X expression during HBV replication and uncertainty concerning its detection have greatly hampered its biochemical and functional characterization. Thus, the cellular distribution of X remains an important and open issue. Several *in vivo* and *in vitro* studies demonstrated X in the nucleus, cytoplasm, or both (Siddiqui *et al*., 1987; Schek *et al*., 1991; Klein *et al*., 1991; Renner *et al*., 1995; Dandri *et al*., 1996). In a recent study, X appeared as a nucleocytoplasmic protein that exerts different effects depending on its location (Doria *et al*., 1995)

In view of these conflicting data and the significance of X for the biology and pathogenesis of HBV, we have re-examined its subcellular location using the following approaches: (1) Analysis of the cell cycle association of X expression and cellular distribution by indirect immunofluorescence in synchronized hepatic cells stably expressing X. (2) Analysis and characterization of X expression and its dynamic localization in living cells using the reporter molecule green fluorescence protein (GFP).

We show that, independently of the cell cycle, the HBV regulatory protein X is in the cytosolic compartment where it colocalizes with the proteasome. Despite its short half-life, this colocalization is not merely the reflection of its proteolysis by the proteasome, since its level does not significantly increase in the presence of the proteasome inhibitor ALLN. Rather, by interacting with the proteasome, X could modulate its activity. In accordance with this hypothesis, we demonstrate that X slows down markedly the proteasome-dependent processing of the NF-$\kappa$B1 precursor protein, p105 to NF-$\kappa$B p50 and stabilizes a C-terminally truncated intermediate. Collectively, our data suggest that X might target proteasomes as one of the most critical protein degradation pathways to subvert cellular functions.

## Results

### *X is retained in the cytoplasm irrespective of the cell cycle*

To study the subcellular distribution of X, we have taken advantage of a previous study from our group on the role of spliced HBV RNAs. We were able to show accumulation of X transcripts in an Huh7 cell line stably transfected with a full length HBV genome and a cDNA corresponding to the 2.2 kb singly spliced HBV RNA (Rosmorduc *et al*., 1995). Using indirect immunofluorescence X was localized in the cytoplasm of these cells where it showed a fine granular to diffuse distribution (Figure 1). The putative cell cycle dependent variation in the expression and localization of X was subsequently analysed using synchronized cell populations. Synchronization was achieved using TGF$\beta$1, double thymidine block, or nocodazole (Figure 1). Cells stably expressing X responded to TGF$\beta$1 treatment with a block in late G1. An early S-phase block could be induced by double thymidine treatment. Finally, nocodazole, a potent inhibitor of tubulin polymerisation, arrested cells efficiently in prometaphase (G2), when the nuclear membrane disassembly occurs (data not shown). At different phases of the cell cycle X did not show any significant changes in its distribution pattern (Figure 1). In summary, in this system X is retained in the cytoplasm and does not translocate into the nucleus during the cell cycle.

### *X shows a punctuate cytoplasmic distribution and associates with the nuclear membrane*

To determine the behaviour of X in living cells and extend it biological characterization, the reporter gene GFP was added to the 3′ end of the X gene (X-GFP) (Figure 2).

We first tested the biological activity of the fusion protein. Chang cells were transfected with the NF-$\kappa$B-LUC reporter gene and expression vectors encoding either X, X-GFP or X-NLS and assayed for luciferase activity. X-GFP fusion protein stimulated NF-$\kappa$B-dependent transcription to the same extent as the untagged (Figure 3, panel b) or flag-tagged X (data not shown). Thus, the C-terminal conjugation of GFP to X does not interfere with its biological activity. X containing the NLS-sequence failed to stimulate NF-$\kappa$B-directed transcription (Figure 3, panel b). The expression of the native X and X-GFP fusion proteins were confirmed by immunoblotting of extracts of transfected Chang cells using a polyclonal rabbit antibody to X (Figure 3, panel a). Despite the fact that the expression of X and X-GFP was under the control of the same promoter (see 'Plasmid Constructs' in Materials and methods), X-GFP fusion protein appeared to accumulate to higher levels than X. This is in contrast to the immunofluorescence data, which show that X and X-GFP accumulated to comparable levels *in situ* (Figures 5 and 6). However, determination of the solubility of X in different buffer conditions revealed that the addition of the GFP-tag enhances its hydrophilicity, accounting for the phenomenon described above (data not shown).

Next we tested the use of GFP as a reporter gene in living cells and compared the intracellular distribution of GFP to that of GFP-Δc-*jun*, X-GFP, X, X-Flag and X-NLS upon transfection of Chang liver cells. Cells expressing GFP alone displayed diffuse fluorescence throughout the cytoplasm and nucleus (Figure 4, panel a) (Chalfie *et al*., 1994). The presence of GFP in both cellular compartments suggested also that specific localization of a fusion protein in either one of these compartments would be meaningful. Indeed, cells transfected with GFP-Δc-*jun* showed an accumulation of fluorescence in the nuclei of interphase cells and resembled cells observed by conventional immunofluorescence technique (Figure 4, panel b) (Ham *et al*., 1995). X-GFP showed a discrete granular appearance (Figure 4, panel c) and the well-defined X-containing foci were distributed throughout the cytoplasm. Thus, in contrast to GFP alone or GFP-Δc-*jun*, X-GFP was specifically localized in the cytoplasm. Identical results were obtained after the transfection of other cell lines,

including Huh7 (Figure 8, panel b), HepG2 and NIH3T3 cells (data not shown). These observations validate the use of GFP as a reporter molecule to study X distribution in living cells, and were reinforced by the identical distribution of X-GFP compared to X-Flag or unmodified X (Figure 5, panels a and b), (Schek *et al*., 1991; Doria *et al*., 1995). Addition of NLS-motif to X resulted in its accumulation as granular structures in the nuclei of transfected Chang cells (Figure 5, panel c).

To study precisely the cellular compartmentalization of X, we have visualized the nuclear membrane of Chang cells transfected with X-GFP using antibodies to Lamin (Figure 6, panel a) and nuclear pore complex (NPC) (Figure 6, panel b) and cells were scanned in horizontal planes of 0.3 $\mu$m thickness by confocal laser microscopy (Figure 6, panels a: 1 through 16 and b: 1 and 5). X expression was characterized by granules randomly distributed in the cytoplasm. However, in a few cells, horizontal sections could not unequivocally

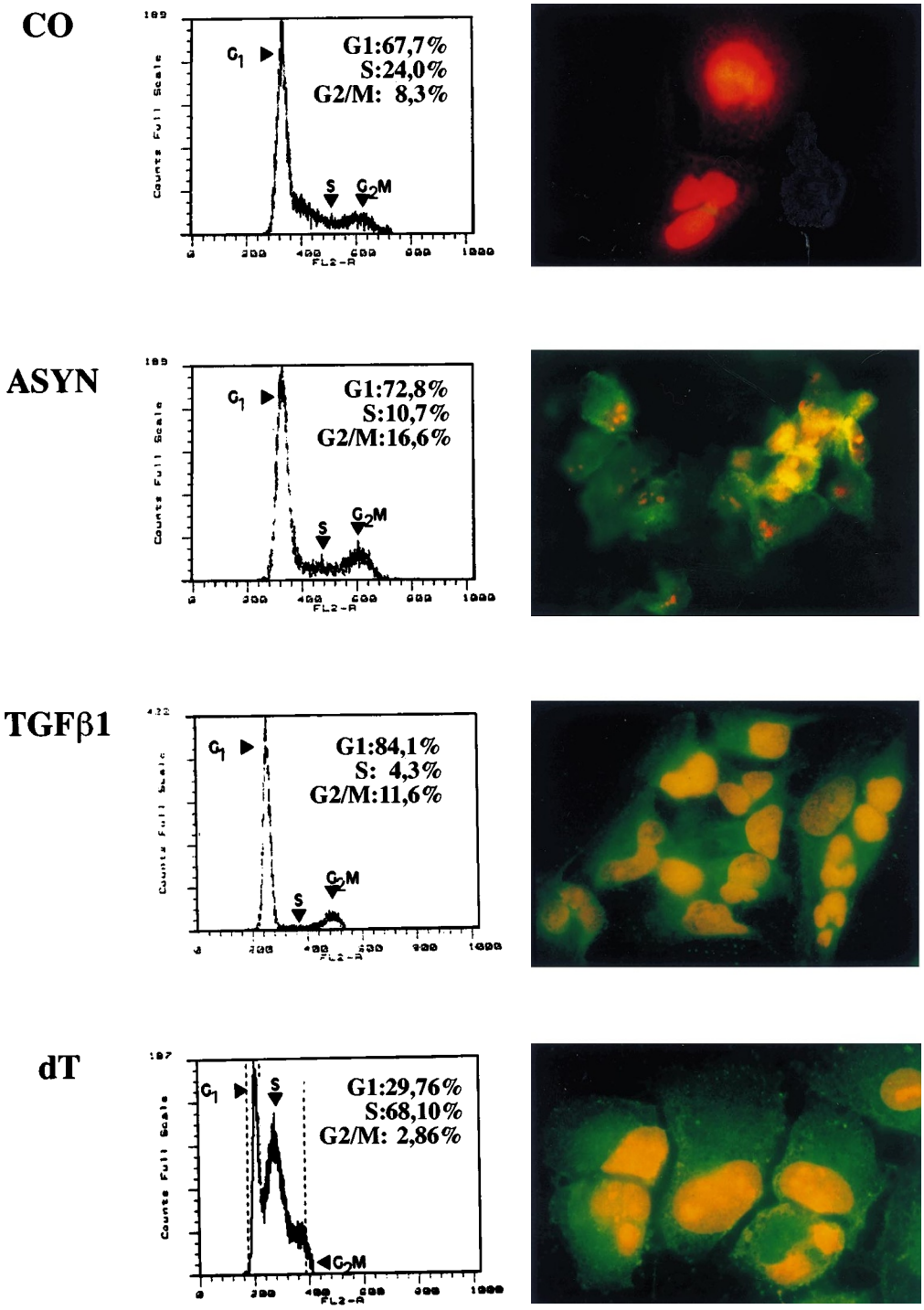


**Figure 1** Cell cycle synchronization and indirect immunolocalization of X. Left panel: Analysis of cell cycle distribution of parental Huh7 cells (Co) and Huh7 cells stably expressing X before (asyn.) and after treatment with TGF$\beta$1 and thymidine (dT) by flow cytometry. The two peaks represent G1 Phase (2n DNA content) and G2/M phase cells (4n DNA content). Right panel shows the distribution of X (green) in the corresponding asynchronous and treated cells. Co corresponds to non-transfected and asynchronous parental Huh7 cells. Nuclei were counterstained with propidium iodide (red)

exclude a potential nuclear localization of single granules (Figure 6, panels a and b: arrowheads and xy). Additional transversal scans revealed that X was indeed not intranuclear and associated firmly to the nuclear membrane (Figure 6, panels a and b: xz).

In summary, X is principally localized in discrete cytoplasmic foci and a fraction of it is attached to the nuclear membrane.

### *X colocalizes* in vivo *with the proteasome*

In order to further characterize the cytoplasmic distribution of X, we have performed double labeling studies using antibodies specifically recognizing different structures of the cytoplasm (Figure 7). There was no evidence for an association of X with components of the cytoskeleton, namely α-tubulin (Figure 7, panel d) or actin (data not shown) nor with the endoplasmic reticulum (Figure 7, panel a). The punctuate pattern of X was reminiscent of lysosomes and endosomes. However, the distribution pattern of these organelles was distinctly different from that of X (Figure 7, panel c). Since heat shock proteins (HSP) are major cellular constituents involved in many processes (for a review, see Freeman and Morimoto, 1996), we asked whether X is associated with HSP70 and 90. However, the distribution of HSP did not significantly coincide with that of X either (Figure 7, panel b).

Subcellular distribution of proteasomes in the human hepatoma cell line Huh7 was studied by indirect immunofluorescence using the MCP II antibodies. Proteasomes are spread diffusely throughout the entire cell (Figure 8, panel a). The cytoplasm exhibits a diffuse staining with perinuclear accentuation, while the nuclei are more abundant for proteasomes and nucleoli are virtually devoid of any labeling. This is in agreement with previous reports showing its nucleocytoplasmic distribution. (Amsterdam *et al*., 1993; Peters *et al*., 1994; Pitzer *et al*., 1996). Immunofluorescence analysis of proteasome distribution in cells expressing X revealed colocalization between X and cytosolic proteasomes (Figure 8, panel b). This was confirmed and detailed by confocal analysis using single channel acquisition for each of the fluorochromes on individual scans (Figure 8, panel c) and cytometrical analysis (Figure 8, panels d and e). Thus, X induced a redistribution of a fraction of the cytoplasmic fraction of proteasomes along the X granules, a pattern absent in non-transfected cells.

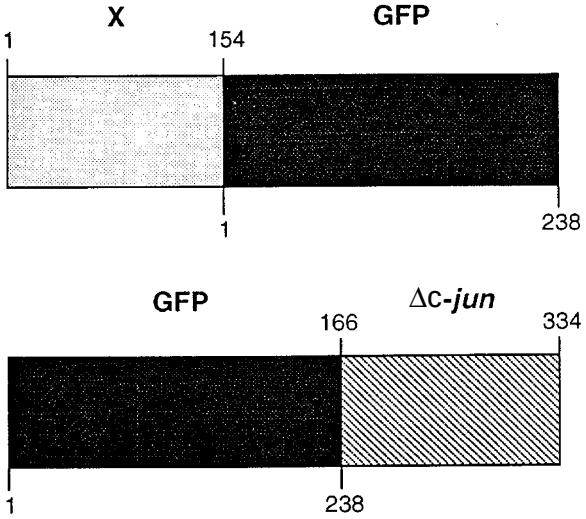


**Figure 2** Diagram of fusion proteins in which X (dotted) or Δc-*jun* (hatched)-sequences are linked in frame to that of the green fluorescence protein (GFP) (filled)

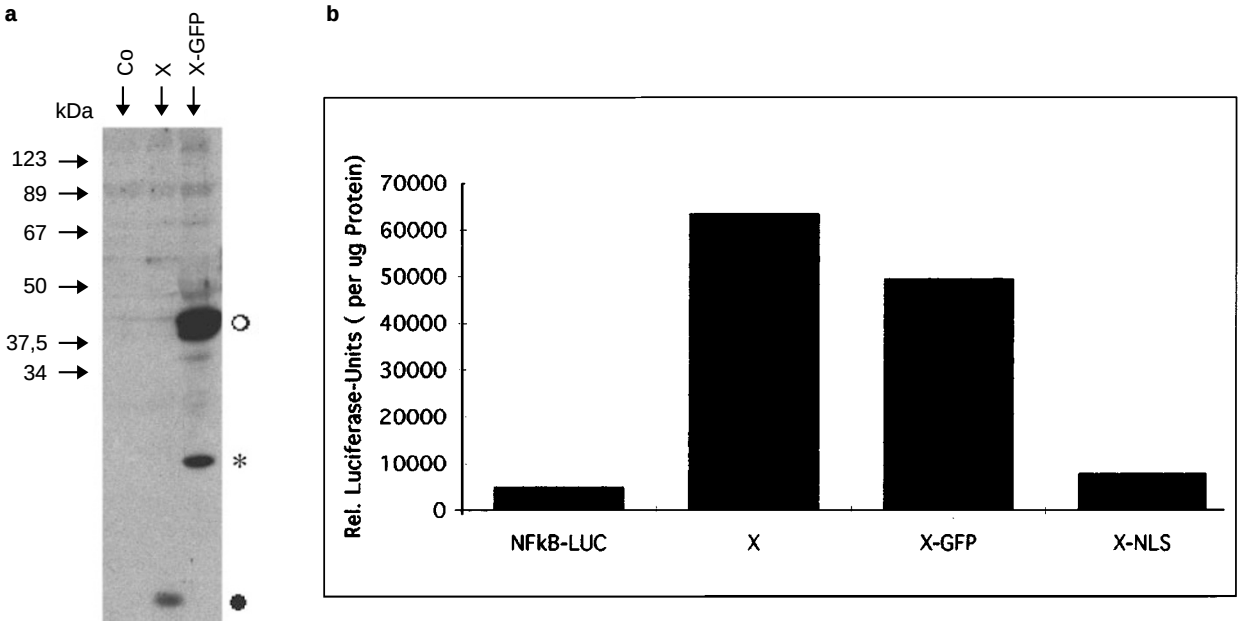


**Figure 3** Panel **a**: Western blot analysis of Chang cells transiently expressing X or X-GFP fusion protein. Chang cells were transfected with 10 μg of X or X-GFP encoding plasmids. Extracts were prepared 36 h later, lysed in Laemmli buffer and subjected to SDS–PAGE. The immunoblot was probed with the polyclonal anti-X serum. Co corresponds to non-transfected cells. The position of X and X-GFP are shown by an open and filled circle, respectively. Asterix points to a degradation product. Panel **b**: Stimulation of NF-κB-dependent transcription by X and X-GFP. Chang liver cells were transiently cotransfected with a NF-κB-LUC reporter plasmid and a vector encoding X, X-GFP or X-NLS. The luciferase activity in the cellular extracts was determined 36 h later. A representative experiment in duplicate is shown (the standard deviation was less than 10%)

In order to determine the half-life of X, Chang cells transfected with X-GFP were pulse-labeled with $^{35}$S-methionine and -cysteine. As shown in Figure 9, the NP-40 soluble fraction of X decays rapidly. To test whether the colocalization of X with the proteasome reflects its degradation pathway, the proteasome inhibitor ALLN was included in the medium during the 1 h pulse period and for the whole duration of the chase. The rapid turnover of X was not markedly affected by the inhibition of the proteasome function (Figure 9). The activity of the proteasome inhibitor was confirmed by the efficient inhibition of TNF-$\alpha$ induced degradation of the I$\kappa$B$\alpha$ which is known to be degraded by the proteasome (data not shown).

In summary, X is located in the cytosol and does not appear to be associated with those organelles and cytoskeletal components so far tested. In contrast, our data have demonstrated the codistribution of X with proteasomes, which does not solely indicate the degradation pathway of X.

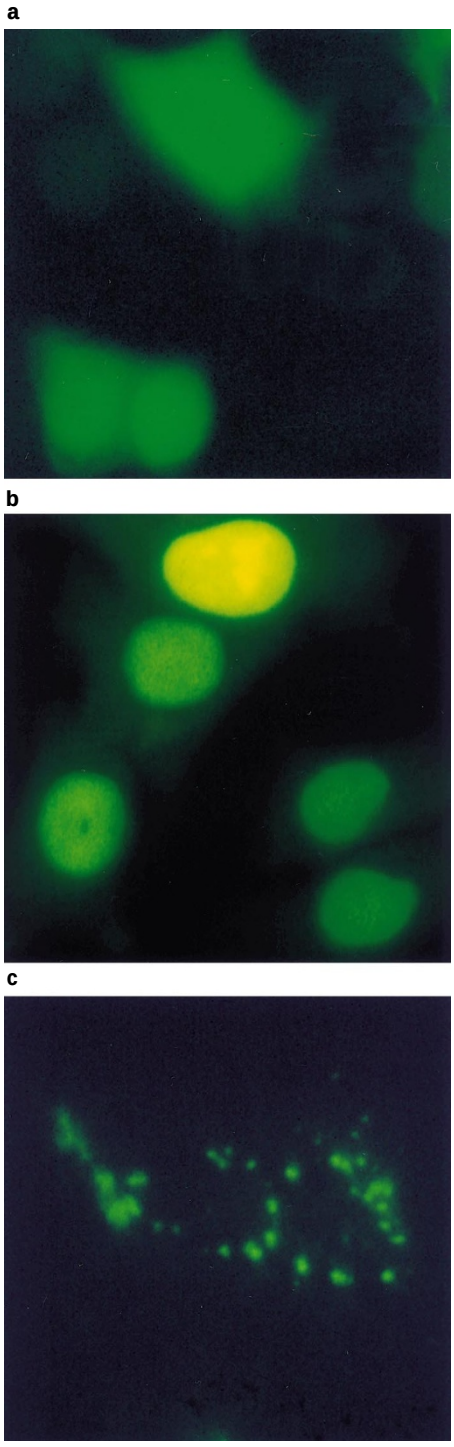


**Figure 4** Distribution of GFP and corresponding fusion proteins in living cells. Chang liver cells were transfected with plasmids encoding: GFP (panel **a**), GFP-Δc-*jun* (panel **b**), or X-GFP (panel **c**). The localization of GFP and of conjugates was observed and photographed using an epifluorescence microscope

### *X slows down the proteolytic generation of NF-κB p50 from its precursor p105*

To demonstrate the functional relevance of the association between X and the proteasome we decided to investigate the effect of X on the processing of the p105 precursor of the p50 subunit of NF-$\kappa$B. Since the processing of p105 has been shown to be dependent on proteasomes (Palombella *et al*., 1994), we have examined the effect of X on this processing. We performed a direct immunoblotting experiment on cell extracts using either an antibody recognizing both p50 and p105 (Figure 10, panel a, lanes 1–4; antiserum 1141) or an antibody raised against the C-terminal region of p105 which consequently recognizes only p105 (Figure 10, panel a, lanes 5–8; antiserum 1140). Transfection of an expression vector encoding X-GFP resulted in a moderate reduction in the level of expression of endogenous p50 (compare lane 2 with lane 1). This is however an underestimation due to the fact that not all the cells are transfected. Because p105 level is very low in Chang cells (Figure 10, panel a, lanes 1, 2, 5, 6), we measured the effect of X on exogenous p105. Transient transfection of an expression vector encoding the full length p105 resulted in its physiological processing into p50 (lane 3). However, co-expression of X and p105 resulted in a 50% decrease in the generation of p50 from p105 (lane 4). In the presence of X, we also reproducibly notice the stabilization of an intermediate molecule reacting with the N-terminal, but not the C-terminal p105 antiserum, which thus represents a C-terminal degradation product (compares lanes 3, 4 and 7, 8). Comparison of lanes 7, 8 with lanes 3, 4 indicates that the major effect of X is in the accumulation of partially processed products and not of full length p105. From this experiment we conclude that X impairs p105 processing and seems to stabilize a C-terminally processed intermediate molecule.

We next confirmed the effect of X on p105 processing by analysing the nuclear DNA-binding activities following transfection of p105 with or without X (Figure 10, panel b). Most of p50 generated from p105 is retained in the cytoplasm through interaction with non-processed p105 (Henkel *et al*., 1992; Rice *et al*., 1992). Therefore the amount of p50 homodimers in the nucleus will depend on the balance between p105 and p50. If there is more p50 than p105 (Figure 10, panel b, lane 3), DNA binding by the p50 homodimer will be detectable as confirmed by shifting with specific antisera (Figure 10, panel b, lane 9). If the processing of p105 is inhibited to such an extent that more p105 than p50 is present, then no nuclear DNA binding by the p50 homodimer should be detectable. This is what happens in the presence of X (Figure 10,

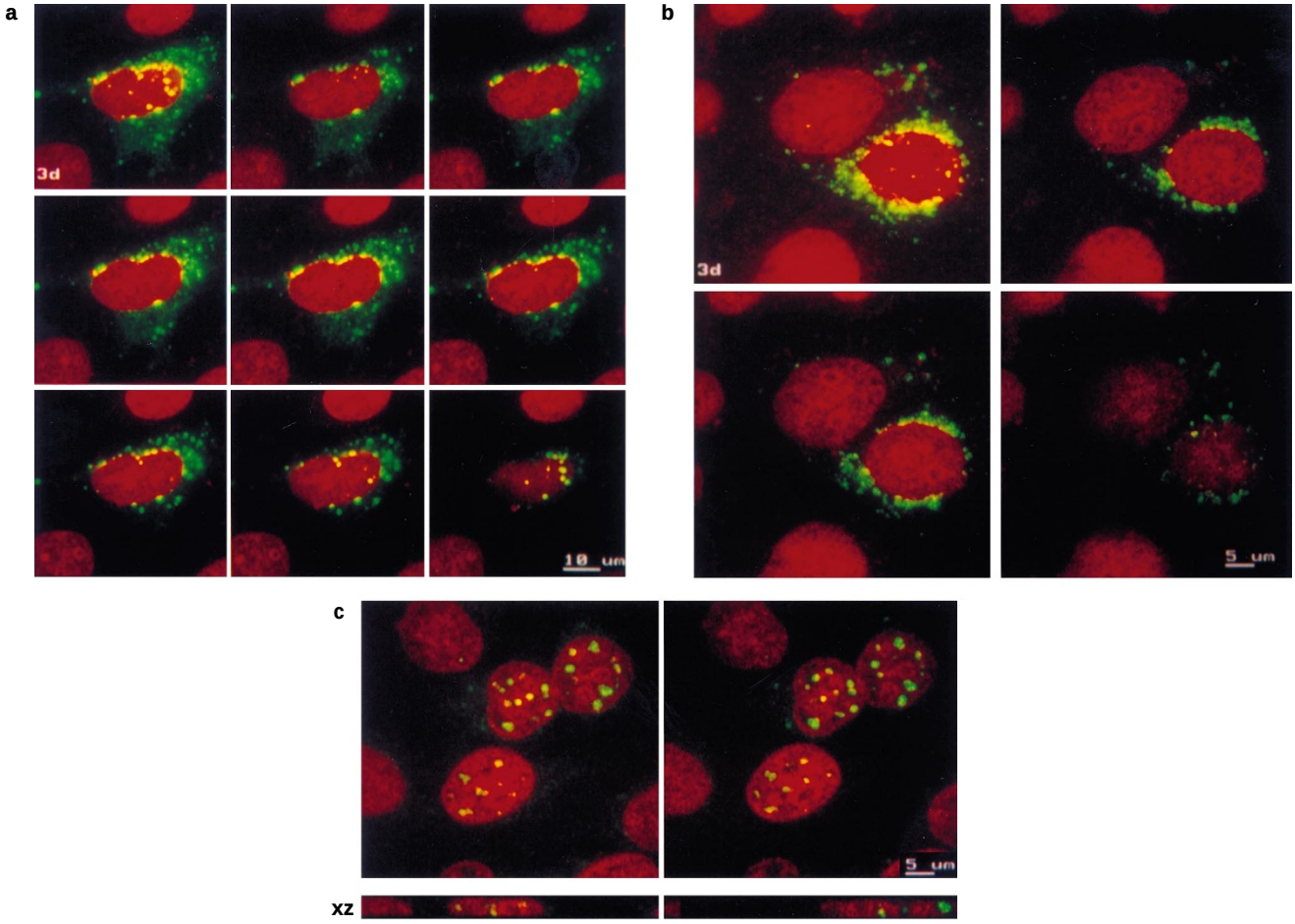


**Figure 5** Confocal microscopic analysis of the cellular distribution of X-Flag (panel **a**), X (panel **b**) and Flag-X-NLS (panel **c**). Chang cells were transfected with the corresponding constructs, fixed 36 h after the transfection and immunolabeled using antibodies to flag-tag (panels **a** and **c**) and X (panel **b**) (green). The nuclei were counterstained with the DNA-binding dye 7-AAD (red). Serial z scans through the whole cells are shown together with the corresponding three dimensional reconstructions (3d). xz in panel **c** represents vertical section

panel b, lane 4). Besides the complex observed in panel b, lane 2 confirms the induction of p50/p65 complexes by the X protein alone (compare lane 2 with lane 1) as recently reported (Chirillo *et al*., 1996; Su and Schneider, 1996). The disappearance of the p50/p65 complex in panel b, lane 4 is due to the presence of an excess of unprocessed p105 which retains both p65 and p50 in the cytoplasm.

## Discussion

In the present study we have examined the cellular distribution of X and its putative cell cycle dependency. We provide data defining the cytosol as the principal compartment of X and showing its codistribution with the proteasome. The functional relevance of this association is substantiated by demonstrating modulation of a proteasome-dependent biological activity by X.

HBV X protein exerts multiple cellular effects, but their relevance to the viral life cycle and potentially malignant conversion of hepatocytes remains elusive. Moreover characterization of the biochemical properties and cellular partners of X is still at an early stage. One of the confusing issues has been so far the uncertain cellular distribution of X. In the present study, we have found that X is mainly retained in the cytosol and this result concurs with several *in vitro* and *in vivo* studies (Siddiqui *et al*., 1987; Schek *et al*., 1991; Klein *et al*., 1991; Renner *et al*., 1995; Dandri *et al*., 1996). In particular, the recent study from (Doria *et al*., 1995) described the nucleocytoplasmic localization of X granules and emphasized the correlation of its distribution with distinct functions. However, our results do not show any nuclear localization of X. The reasons for this discrepancy are not clear, since both studies used a combination of Chang liver cells and transient expression of X. They might be due in part to methodological caveats. Doria *et al*. used coexpressed EBNA-1 to visualize the nuclear boundaries. However, EBNA-1 distribution does not strictly reflect the boundaries of the nucleus. The use of NPC and/or Lamin as precise markers of the nuclear membrane (NM), has permitted the demonstration of association of X with the nuclear membrane (Figure 6). Thus, the close attachment of X to the nuclear membrane may be responsible for its detection in the nuclear fractions (Schek *et al*., 1991; Siddiqui *et al*., 1987).

In view of a transcriptional activator function for X (for a review, see Yen, 1996; Hildt *et al*., 1996) one might expect a modulation of its expression and cellular distribution during the cell cycle. However,

we did not observe any change in the distribution pattern of X in our stable clone, indicating that it acts primarily in a compartment external to the nucleus (Figure 1). However, we cannot exclude that X may interact with cellular factors induced or activated upon cellular stimulation by growth factors and cytokines, and translocates subsequently into the nucleus. We can also not exclude low, but undetectable amounts of nuclear X by means of techniques used so far.

In this study we demonstrate the codistribution of X with the cytosolic fraction of proteasomes. This result is consistent with recent data obtained from yeast two-hybrid studies showing an interaction of X with a novel α-subunit, XAPC7, of the 20S proteasome

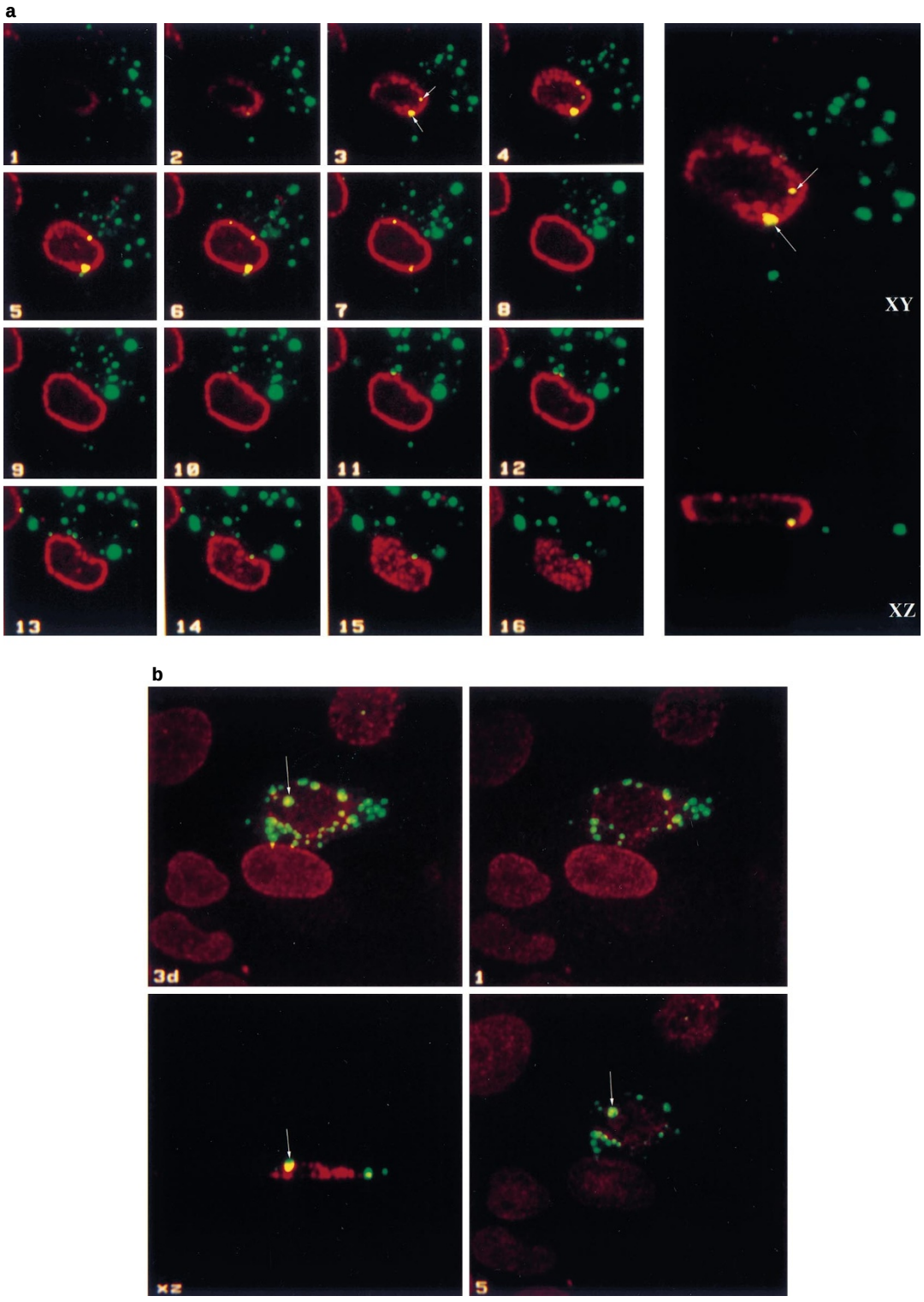


**Figure 6** Subcellular distribution of X by scanning confocal microscopy. Chang liver cells were transfected with the X-GFP construct, fixed and immunolabeled as follows: panel **a** immunostaining for Lamin as a nuclear membrane marker (NM). Images were scanned on two channels (red for Lamin and green for X-GFP). Serial horizontal sections extending from the bottom to the top of the same cell are shown on the left. The right panel shows an additional horizontal (xy) and vertical (xz) scan of the same cell. Arrows point to the X granules associated with NM. Panel **b** provides a further example of the close attachment of X (green) to the NM evidenced by nuclear pore complex-(NPC) immunostaining (red). From the same cell, 3D-reconstruction (3d) and two selected horizontal scans (1 and 5) are shown in addition to the vertical section (xz). The arrow points to a X-granule with a pseudonuclear localization

(Fischer *et al*., 1995; Huang *et al*., 1996). Genetic analysis identified both a middle domain and the C-terminal 20 amino acids of XAPC7 as essential for binding with X (Huang *et al*., 1996). However, in both studies demonstration of the *in vivo* association of X to the identified subunit could not be achieved. Such

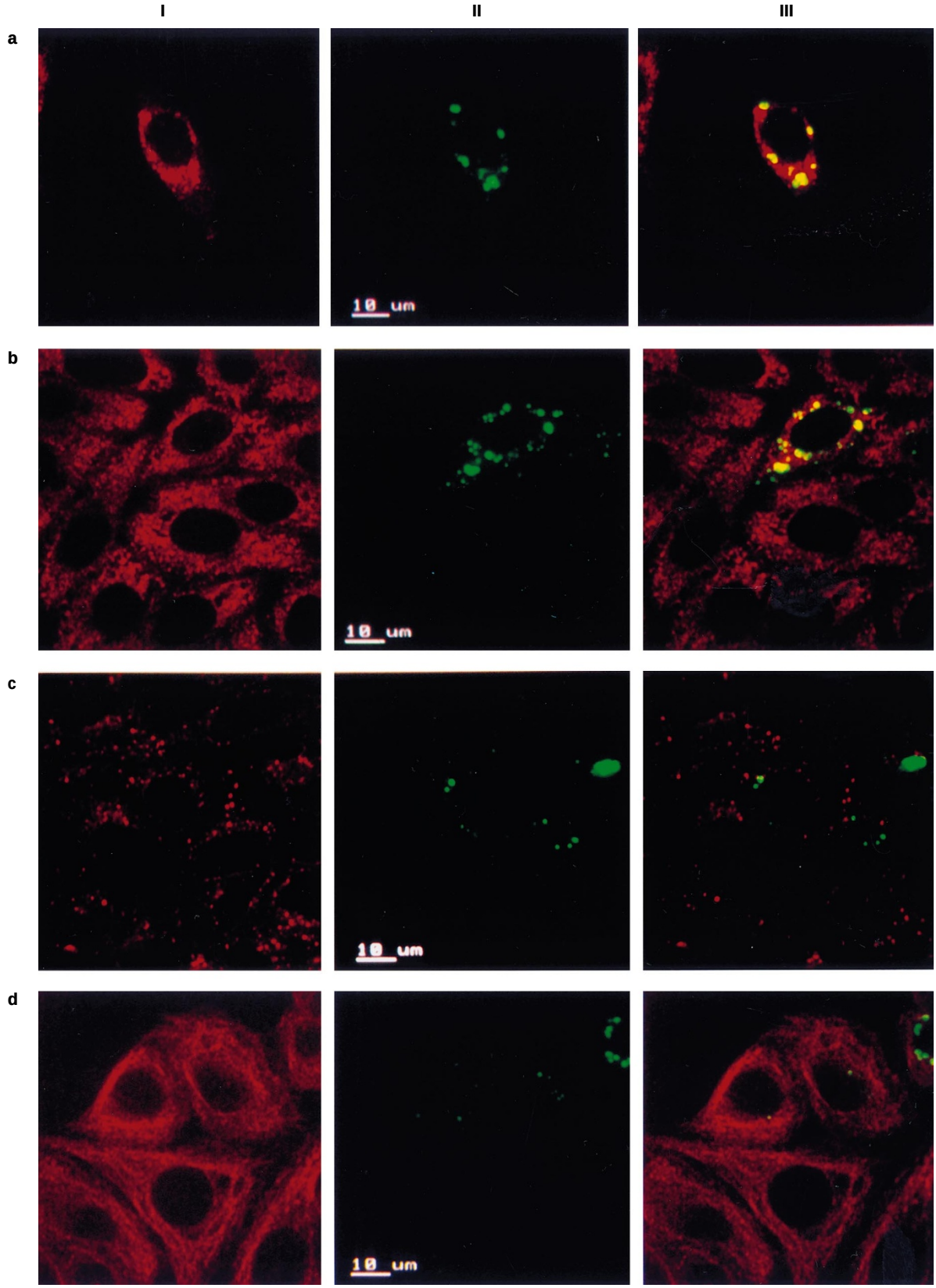


**Figure 7** Analysis of the cytoplasmic distribution of X in cells immunolabeled for the following cytoplasmic structures: endoplasmic reticulum (panel **a**), HSP 90 (panel **b**), endosomes/lysosomes (panel **c**) and α-tubulin (panel **d**). Chang liver cells were transfected with the X-GFP expression vector and cells were indirectly immunostained for the indicated cellular structures. Each panel shows reconstructions of horizontal confocal scans of cytoplasmic marker alone (I), X-GFP alone (II) or distribution of both fluorochromes merged to a single projection (III)

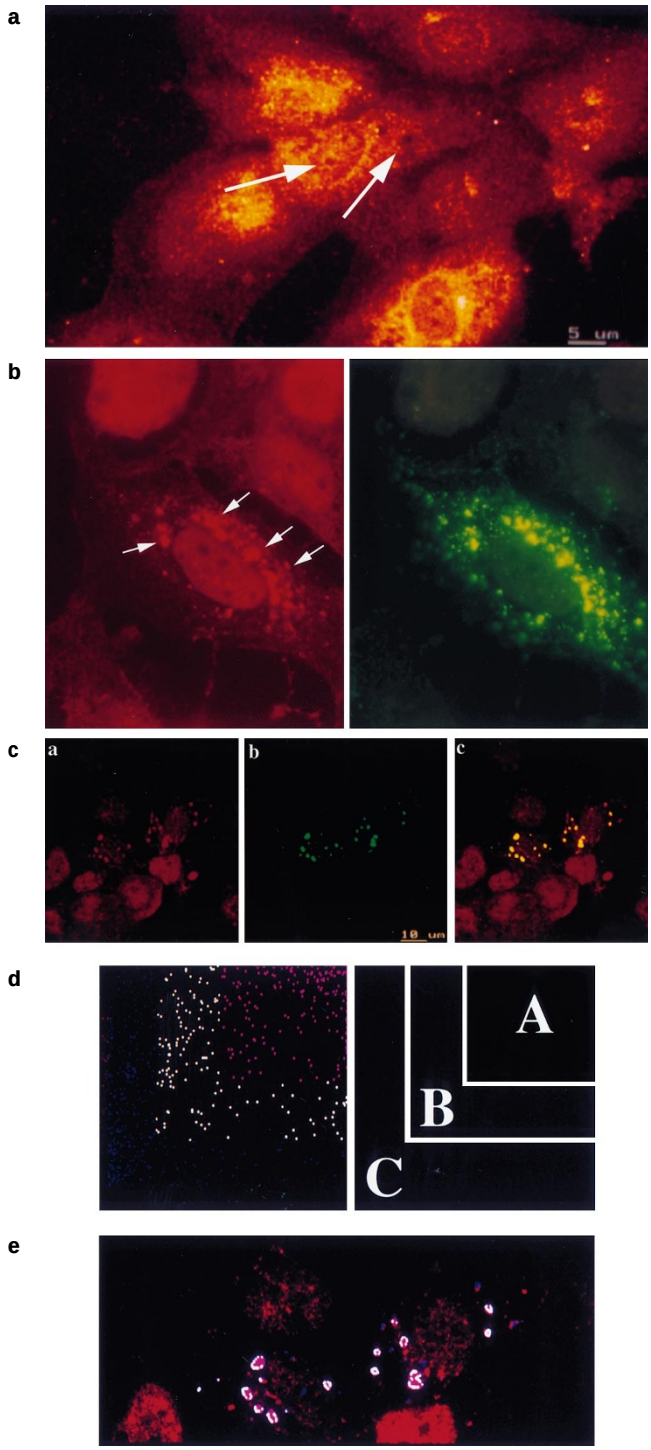


**Figure 8** Colocalization of X and proteasomes. Huh7 cells were transfected with the X-GFP construct (green) and immunostained for proteasomes using MCP II antiserum (red). Panel **a** shows the distribution of proteasomes in non-transfected Huh7 cells by confocal microscopy. Arrows point to nucleoli and cytoplasmic vacuoles devoid of any staining. Panel **b** shows the epifluorescence micrograph of Huh7 cells expressing X-GFP (green) and immunostained for proteasomes (red). Note the granular clustering of cytosolic proteasomes along the X granules (Arrows). Panel **c** represents a reconstruction of serial confocal scans through the same cells. Areas of coincidence of red and green fluorescence (yellow) indicate overlapping distribution of X and proteasomes. Panel **d** shows cytofluorographic distribution of red and green fluorescence intensities. The cytofluorogramm was divided in three arbitrary regions (squares A–C) in order to obtain the most stringent correlation between the spatial distribution of X and proteasomes whereas A contains the most intense pixels for green and red fluorescence. Panel **e** shows the numerical image resulting from the cytometrical calculations for region A in panel **d**

difficulties are likely, at least in part, to be due to the fact that the interaction between X and proteasome might not be stringent enough to be maintained during the immunoprecipitation. Thus, our results demonstrate for the first time the *in vivo* colocalization of X with the proteasome. Proteasomes are very abundant in cells and play an essential role in regulation of the cell cycle, apoptosis, signal transduction and immune responses (for a review, see Coux *et al*., 1996; Baldwin, 1996). Since X is a short lived protein (Schek *et al*., 1991), (Figure 9) and proteasomes eliminate such proteins (Glotzer *et al*., 1991; Henkel *et al*., 1993; Maki *et al*., 1996; Rock *et al*., 1994; Trier *et al*., 1994), this interaction could simply indicate the degradation of X. However, in pulse-chase experiments, X turns over rapidly (Figure 9) (Schek *et al*., 1991) and its decay is not modified by inhibition of the proteasome (Figure 9). Such a rapid turnover could explain the low levels of X during HBV infection. To test the possibility that X might alter the function of the proteasome, we have studied a protein whose major biological effects are depending on its processing by the proteasome: proteolytic maturation of the p105 precursor of the p50 subunit of NF-$\kappa$B occurs constitutively at a slow rate, and degradation is limited to the C-terminal half of the protein, whereas the N-terminal portion (p50) is left intact (Palombella *et al*., 1994). The presence of X decreased the generation of p50 from p105, and stabilized an intermediate molecule representing a C-terminal degradation product (Figure 10, panel a). Consequently, X decreased also the nuclear DNA binding activity of p50 homodimers generated from p105 (Figure 10, panel b). Therefore our study shows a modification of a proteasome-dependent biological activity upon X expression, and thus substantiates the

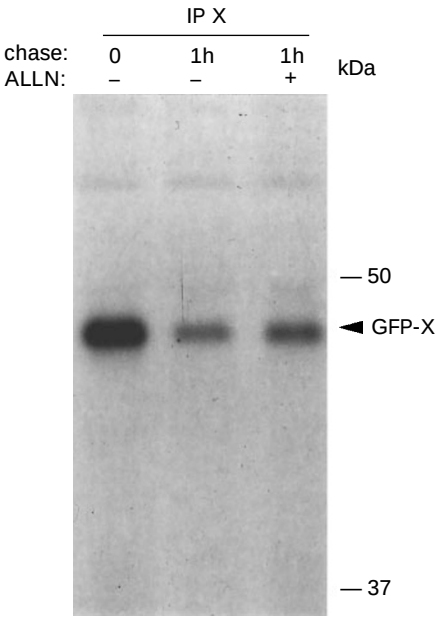


**Figure 9** Kinetics of turnover of X. Chang cells transfected with X-GFP encoding vector were pulsed for 1 h as indicated in Material and methods and chased with cold medium in the absence or presence of ALLN. Total cell lysates were immunoprecipitated with the rabbit anti-X antiserum and fractionated by SDS–PAGE. The arrow indicates the position of the X-GFP fusion protein. IP: immunoprecipitation for X

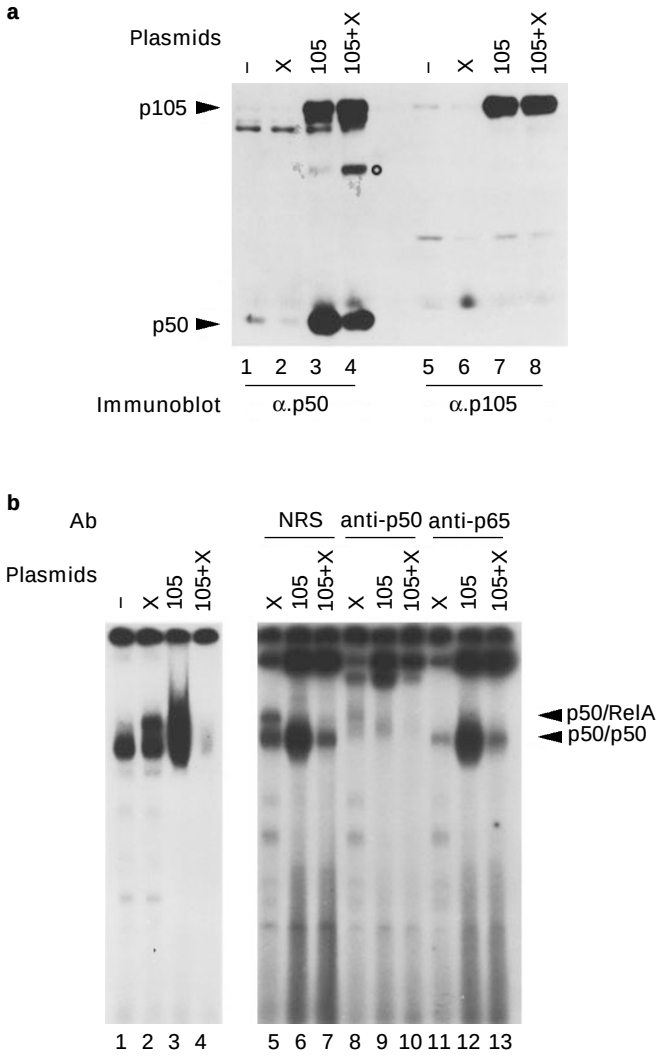


**Figure 10** Panel **a**: Impairment of processing of transfected p105 by X in Chang cells. 50 $\mu$g of whole cell lysates from Chang cells non transfected or transfected either with X-GFP, p105, or both were subjected to immunoblot analysis using anti-p105/p50-serum 1141 (lanes 1–4) or anti-p105-serum 1140, (lanes 5–8). The position of p105 and p50 are shown by arrows and the presence of a degradation product is marked by a circle (○). Panel **b**: X inhibits the appearance of nuclear p50 homodimers. Chang cells were transfected with either X-GFP, p105 or both. After 36 h, nuclear extracts were prepared and bandshift assays were performed as indicated in Materials and methods. A portion of these extracts (5 $\mu$g for lanes 1, 2, 5, 8, 11; 0.25 $\mu$g mixed with 5 $\mu$g BSA for lanes 3, 4, 6, 7, 9, 10, 12, 13) was directly subjected to EMSA, or preincubated with antibodies (normal rabbit serum (NRS), lanes 5–7; anti-p50, lanes 8–10; anti-p65, lanes 11–13) before EMSA. Arrowheads indicate the position of bands corresponding to p50-homo- and p50/p65-heterodimers

functional significance of this colocalization. At first sight this result might appear paradoxical in the light of the well documented activation of NF-$\kappa$B by X (Chirillo *et al*., 1996; Su and Schneider, 1996) confirmed by the induction of nuclear, p50/p65 containing, NF-$\kappa$B complexes upon X expression (Figure 10, panel b). Thus, the relevance of this impairment of the p105 processing to X-mediated NF-$\kappa$B activation is currently unclear, although transcriptional repression activity has sometimes been assigned to p50 homodimers. Altogether the data presented suggest that X triggers NF-$\kappa$B activation by an alternate mechanism that might or not be related to its codistribution with proteasomes. We are currently investigating the details of this mechanism. Interestingly, another non-DNA binding viral transactivator the HTLV-1 encoded Tax protein seems to display different effects than X on p105 processing (Rousset *et al*., 1996), while HIV-1 Tat protein has been shown to inhibit the proteolytic activity of the 20S proteasome by binding to both 20S and 19S complexes and it is not known how this is related to activation of NF-$\kappa$B (Nelbock *et al*., 1990; Seeger *et al*., 1997). This emphasizes the various strategies designed by viruses to subvert cellular functions. The reported interaction of X with the XAPC7 $\alpha$-subunit, which resides in close neighbourhood to the annulus of the proteasome, might interfere with the proper opening of the external $\alpha$-ring, entry of the protein substrates and subsequent proteasomal processivity, leading to generation of larger intermediates (Huang *et al*., 1996; Goldberg *et al*., 1997; Groll *et al*., 1997). An alternative non mutually exclusive hypothesis is that X may remodel the proteasome by changing its composition, interfering with the NLS-signal of XAPC7 located near the interaction site at the C-terminus (Nederlof *et al*., 1995; Fischer *et al*., 1995; Huang *et al*., 1996). Clearly further work is needed to investigate in detail the precise underlying mechanism(s) and the physiological implication(s) of the X-proteasome interaction.

In summary, our investigation supports the view that HBV X protein is a cytoplasmic regulator capable of modulating a major cellular degradation pathway. The codistribution of X with proteasomes might be one of the pathways used by this viral protein to subvert cellular functions and exert its pleiotropic effects.

## Materials and methods

### *Cell culture*

We used the following cell lines: Hela, Huh7 (derived from a human hepatocarcinoma) and Chang human liver cells (CCl13). Generation and characterization of the Huh7-derived cell line stably transfected with a full length HBV genome and a cDNA corresponding to the reverse transcribed 2.2 kb singly spliced HBV DNA and expressing X has been described previously (Rosmorduc *et al*., 1995). All cell lines were propagated in Dulbecco's modified Eagle's medium (D'MEM) (Gibco Technologies) supplemented with 10% fetal calf serum (FCS).

### *Plasmid constructs*

The GFP-cDNA was cloned into the expression vector pcDNA3 (Invitrogen). To obtain X-GFP fusion protein, X sequence from pTHBV1.3 (a generous gift from Dr H Schaller, ZMBH, Heidelberg) (Guidotti *et al*., 1995) was amplified by PCR using the following primers: 5′-GCGAAGCTTCGTTTCCATGGCTGCTAGGCT3-3′, containing a *Hind*III restriction site and 5′-GCG-GTCGACGGCAGAGGTGAAAAAGTTGCA-3′, which contains a *Sal*I restriction site replacing the stop codon TAA of the X gene. The amplified insert was cloned downstream of the CMV promoter via the *Hind*III and *Sal*I restriction sites linking X in frame to the GFP sequence. The GFP expression vectors used in this study are schematically summarized in Figure 2. To obtain the CMV-X plasmid, X-ORF was subcloned into the expression vector pcDNA3 by PCR. The X-Flag construct has been previously described (Doria *et al*., 1995). The deletion

mutant of c-*jun*-Δ166-334, fused to GFP (GFP-Δc-*jun*) was kindly provided by Dr C Pfarr (Institut Pasteur, Paris) (Ham *et al*., 1995). The construct Flag-X-NLS, contains the nuclear localization signal (NLS) of SV40 Large T-Antigen fused to the C-terminus of X and was kindly provided by Dr M Levrero (La Sapienza, Rom). The NF-κB precursor p105 was expressed from the Rc/CMV (Invitrogen) and has been described previously (Blank *et al*. 1991). Plasmid maps and construction details are available upon request.

*Transfections and luciferase assays*

Transfections were carried out using the calcium phosphate precipitation technique (Rosmorduc *et al*., 1995). Cells were incubated with calcium phosphate/DNA-precipitate (10 μg per 10 cm plate) overnight. Cells were harvested and analysed at time points indicated. For luciferase assays, Chang cells were transfected with 2 μg (per well in a six well plate) of expression vectors as indicated along with 1 μg of a luciferase reporter plasmid driven by -κB consensus sequences (NF-κB-LUC) (Ten *et al*., 1992). The total amount of DNA for each transfection was normalized by addition of sonicated salmon sperm DNA (Promega). At 36 h post-transfection, cells were harvested for luciferase assay (Promega). Luciferase activity is presented as light units/μg protein. Protein concentrations were determined by a Bradford assay (Bio-Rad). Data presented are the mean values of transfections done in duplicate, and the results are representative of three separate experiments.

*Cell cycle synchronization*

Huh7 derived clones were arrested either in prometaphase by a 24 h exposure to 50 ng/ml of nocodazole (Sigma) or in late G1 by a 36 h exposure to 4 ng/ml of transforming growth factor β1 (TGFβ1) (Ozyme), or in early S-Phase using a double thymidine (Sigma) block consisting of 16 h exposure to 5 mM thymidine followed by release for 10 h and re-exposure for 16 h. The cell cycle distribution was analysed subsequently by FACS.

*FACS analysis*

Briefly, cells were trypsinized and fixed with ice-cold 70% ethanol. For DNA content analysis, propidium iodide was added at 40 μg/ml and cells were incubated in the presence of RNase at 100 μg/ml for 30 min at 37°C. DNA-content was determined in a Becton Dickinson FACS II. The percentage of cells in different phases of the cell cycle was calculated using the Cell Fit Program (Becton Dickinson).

*Antisera*

The antisera used were the following: anti-sera raised against a p105 N-terminal peptide (peptide 1141), a p105 C-terminal peptide (peptide 1140 or against p65 peptide 1226) (kindly provided by N Rice, Fredericks, USA). The polyclonal X antibodies were generated by immunization of rabbits using renatured recombinant X protein produced in *E. coli*. Polyclonal antibodies to proteasome (MCP II) have been raised following immunization of rabbits with pure fraction of 20S proteasomes isolated from the granulosa cell line POGRSI (kindly provided by Dr W Baumeister and Dr F Pitzer, Martinsried, Germany). Purification of proteasomes and characterization of the MCP II antibodies have been described elsewhere (Amsterdam *et al*., 1993; Pitzer *et al*., 1996). The following antibodies were also kindly provided: endoplasmic reticulum (D Louvard, Institute Curie, Paris) (Louvard *et al*., 1982), Lamin B (JC Courvalin, Institut Jacques Monod, Paris) (Buendia and Courvalin, 1997) and endosomes/lysosomes (A Dautry-Varsat, Institut Pasteur, Paris) (Duprez *et al*., 1994). Following antibodies and fluorochromes were purchased: antibodies to flag-epitope (Integra Biosciences), to heat shock proteins 70 and 90 (HSP) (Stressgen), to α-tubulin (Boehringer), to nuclear pore complex (Babco), phalloidin-rhodamin-conjugate for direct labeling of actin (Sigma), propidium iodide (Sigma) and 7-Actinomycin D (7-AAD) (Sigma).

*Immunofluorescence*

To label endosomes and lysosomes, X-GFP expressing Chang cells were incubated with transferrin-rhodamine conjugates for 30 min at 37°C and subsequently fixed. For indirect immunofluorescence, cells were plated on glass coverslips and grown for 12–16 h before synchronization or transfection. After the treatment cells were fixed 10 min in acetone/methanol (1:1) at −20°C, or ice-cold 4% paraformaldehyde (Sigma) as specified. Unspecific binding sites were blocked with 10% normal goat serum (Dako). Incubation with primary antibodies was carried out at room temperature for 1 h. The fluorochrome conjugated secondary antibodies (Amersham) were added at room temperature for 30 min. Cell nuclei were counterstained with 7-AAD or propidium iodide. The coverslips were mounted on glass slides with 90% glycerol and the slides were then analysed using an epifluoresence microscope (Zeiss) with appropriate filters or confocal laser microscopy (Leica).

*Cell extracts and immunoblots*

Chang cells ($5 \times 10^6$) were washed once in PBS, and lysed in 250 μl of CHRIS 1X (50 mM Tris (pH 8.0), 10% glycerol, 200 mM NaCl, 0.5% Nonidet P-40 and 0.1 mM EDTA), supplemented with 10 μg/ml each of the following protease inhibitors: leupeptin, aprotinin, N-tosyl-L-phenylalanine chloromethlyl ketone (TPCK), N-p-tosyl-L-lysine chloromethyl ketone (TLCK) and phenylmethyl-sulfonyl fluoride (PMSF) as well as the phosphatase inhibitors sodium fluoride (50 mM) and sodium orthovanadate (1 mM). Following electrophoresis, the proteins (50 μg) were transferred to Immobilon membranes (Millipore) and immunoblots were incubated with blocking buffer (5% milk powder dissolved in TNaCIE (10 mM Tris-HCl (pH 7.5), 50 mM NaCl, 2.5 mM EDTA (pH 8.0)) and then subsequently with the following antibodies: anti-p105 (antiserum 1140) anti-p105/p50 (antiserum 1141), anti-GFP or anti-X diluted 1/1000 Reactive protein bands were visualized using the enhanced chemoluminescence (ECL-Amersham) according to the manufacturers instructions.

*Preparation of nuclear extracts and electrophoretic mobility shift and supershift assay*

Transfected Chang cells were pelleted and solubilized in buffer EMSA I containing 50 mM Tris-HCl (pH 7.9), 10 mM KCl, 1 mM EDTA, 0.2% Nonidet P-40 (NP40), 10% glycerol and supplemented with protease inhibitors (see 'Cell extracts'). The lysates were centrifuged at 6500 *g* for 3 min and the pelleted nuclei were incubated for 20 min at 4°C with buffer EMSA II containing 400 mM NaCl, 20% glycerol, 20 mM HEPES (pH 7.9), 10 mM KCl, 1 mM EDTA and protease inhibitors. The extracts were centrifuged at 14 000 *g* for 10 min and supernatants were immediately frozen in liquid nitrogen and stored at −80°C before use. The following partially double stranded oligonucleotide probe, KBF1, was used for bandshift assays: 5′-GATCTGGGGATTCCCCAT-3′ 3′-ACCCCTA-AGGGGTACTAG-5′.

Mobility shift assay were performed in a total volume of 20 $\mu$l in the following buffer: 10 mM Tris-HCl (pH 8.0), 100 mM KCl, 5 mM $MgCl_2$, 1 mM dithiothreitol, 0.5 mg/ml BSA, 10% glycerol. Each reaction, also containing 1 $\mu$l of the $^{32}$P end-labeled probe and 1 $\mu$g of poly(dI-dC), was initiated by the addition of 5 $\mu$g of nuclear extracts (or, for some indicated experiments, 0.25 $\mu$g of nuclear extract mixed with 5 $\mu$g BSA), and allowed to incubate at room temperature for 30 min prior to electrophoretic analysis on a 5% polyacrylamide gel in 0.5X TBE buffer. For supershift experiments, the reaction was also incubated with 0.5 $\mu$l of anti-serum.

*Metabolic labeling*

Chang cells were transfected with X-GFP encoding construct. Thirty-six h after transfection cells were washed twice with PBS followed by a 1 h preincubation with cystein- and methionine-free D′MEM supplemented with 2% dialysed serum and 1% glutamine. Cells were labeled for 1 h in the same medium with 100 $\mu$Ci/ml of Promix $^{35}$S (Amersham), washed with PBS and refed with D′MEM supplemented with 10% FCS and with 5 mM unlabeled cystein and methionine. At indicated times after pulse, cells were incubated with and without the proteasome inhibitor ALLN at 100 $\mu$M (Sigma). Equal aliquots were lysed in CHRIS 1X (see cell extracts) and labeled X was recovered by immunoprecipitation with polyclonal rabbit X antiserum, separated by SDS–PAGE and detected by autoradiography. As a control for the inhibition of proteasome activity by ALLN, Hela cells were incubated with TNF-$\alpha$ at 100 U/ml in the presence or absence of ALLN for indicated lime points and the induced degradation of the endogenous I$\kappa$B$\alpha$ inhibitor of NF-$\kappa$B was assayed by immunoblotting as described above.

**Acknowledgements**

The excellent technical assistance of R Hellio in confocal microscopy is gratefully acknowledged. We also thank Drs W Baumeister, JC Courvalin, A Dautry-Varsat, M Levrero, D Louvard, N Rice and H Schaller for helpful discussions and for providing expression vectors and antibodies. H Sirma is recipient of a fellowship from the DFG. O Rosmorduc was supported by a grant from CNRS/Assistance Publique de Paris and R Weil is a recipient of a fellowship ANRS (Agence Nationale de Recherche sur le Sida). This work was supported by grants from INSERM, EC, ARC, LNL and CNAM to C Bréchot and from ARC, ANRS, Ligue Nationale contre le Cancer to A Israël.

**References**

Amsterdam A, Pitzer F and Baumeister W. (1993). *Proc. Natl. Acad. Sci. USA,* **90,** 99–103.

Avantaggiati ML, Natoli G, Balsano C, Chirillo P, Artini M, DeMarzio E, Collepardo D and Levrero M. (1993). *Oncogene,* **8,** 1567–1574.

Baldwin A. (1996). *Annul. Rev. Immunol.,* **14,** 649–681.

Beasley R, Lin C, Hwang L and Chien C. (1981). *Lancet,* **2,** 1129–1133.

Benn J and Schneider RJ. (1994). *Proc. Natl. Acad. Sci. USA,* **91,** 10350–10354.

Blank V, Kourilsky P and Israel A. (1991). *EMBO J.,* **10,** 4159–4167.

Buendia B and Courvalin JC. (1997). *Exp. Cell. Res.,* **230,** 133–144.

Chalfie M, Tu Y, Euskirchen G, Ward WW and Prasher DC. (1994). *Science,* **263,** 802–804.

Chen H, Kaneko S, Girones R, Anderson R, Hornbuckle W, Tennant B, Cote P, Gerin G, Purcell R and Miller R. (1993). *J. Virol.,* **67,** 1218–1226.

Cheong J-H, Yi M-K, Lin Y and Murakami S. (1995). *EMBO J.,* **14,** 143–150.

Chirillo P, Falco M, Puri PL, Artini M, Balsano C, Levrero M and Natoli G. (1996). *J. Virol.,* **70,** 641–646.

Colgrove R, Simon G and Ganem D. (1989). *J. Virol.,* **63,** 4019–4026.

Coux O, Tanaka K and Goldberg A. (1996). *Annu. Rev. Biochem.,* **65,** 801–839.

Dandri M, Schirmacher P and Rogler C. (1996). *J. Virol.,* **70,** 5246–5254.

Doria M, Klein N, Lucito R and Schneider RJ. (1995). *EMBO J.,* **15,** 4747–4757.

Duprez V, Smoljanovic M, Lieb M and Dautry-Varsat A. (1994). *J. Cell. Sci.,* **107,** 1289–1295.

Fischer M, Runkel L and Schaller H. (1995). *Virus Genes,* **10,** 99–102.

Freeman B and Morimoto R. (1996). *EMBO J.,* **15,** 2969–2979.

Glotzer M, Murray AW and Kirschner MW. (1991). *Nature,* **349,** 132–138.

Goldberg AL, Akopian TN, Kisselev AF and Lee DH. (1997). *Mol. Biol. Rep.,* **24,** 69–75.

Groll M, Bitzel L, Lowe Y, Stock D, Bochtler M, Bartunik H and Huber R. (1997). *Nature,* **386,** 463–471.

Guidotti L, Matzke B, Schaller H and Chisari F. (1995). *J. Vir.,* **69,** 6158–6169.

Ham J, Babij C, Whitfield J, Pfarr CM, Lallemand D, Yaniv M and Rubin LL. (1995). *Neuron,* **14,** 927–939.

Henkel T, Zabel U, van Zee K, Muller JM, Flanning E and Baeuerle PA. (1992). *Cell,* **68,** 1121–1133.

Henkel T, Machleidt T, Alkalay I, Kronke M and Baeuerle PA. (1993). *Nature,* **365,** 182–185.

Hess J, Stemler M, Will H, Schröder CH, Kuhn J and Braun R. (1988). *Med. Microbiol. Immunol. (Berl).,* **177,** 195–205.

Hildt E, Hofschneider PH and Urban S. (1996). *Sem. Virol.,* **7,** 333–347.

Huang J, Kwong J, Sun EC-Y and Liang TJ. (1996). *J. Virol.,* **70,** 5582–5591.

Kekulé AS, Lauer U, Weiss L, Luber B and Hofschneider PH. (1993). *Nature,* **361,** 742–745.

Klein R, Schröder CH and Zentgraf H. (1991). *Virus Genes,* **5,** 157–174.

Kodama K, Ogasawara N, Yoshikawa H and Murakami S. (1985). *J. Virol.,* **56,** 978–986.

Levrero M, Stemler M, Pasquinelli C, Alberti A, Jean-Jean O, Franco A, Balsano C, Diop D, Bréchot C, Melegari M, Villa E, Barnaba M, Perricaudet M and Will H. (1991). *Hepatology,* **13,** 143–149.

Louvard D, Reggio H and Warren G. (1982). *J. Cell. Biol.,* **92,** 92–107.

Maguire H, Hoeffler J and Siddiqui A. (1991). *Science,* **252,** 842–844.

Maki C, Huibregste J and Howley P. (1996). *Cancer Res.,* **56,** 2649–2654.

Nederlof PM, Wang HR and Baumeister W. (1995). *Proc. Natl. Acad. Sci. USA,* **92,** 12060–12064.

Nelbock P, Dillon PJ, Perkins A and Rosen CA. (1990). *Science,* **248,** 1650–1653.

Palombella VJ, Rando OJ, Goldberg AL and Maniatis T. (1994). *Cell,* **78,** 773–786.

Persing D, Varmus H and Ganem D. (1986). *J. Virol.,* **60,** 177–184.

Peters J-M, Franke WW and Kleinschmidt JA. (1994). *J. Biol. Chem.,* **269,** 7709 – 7718.
Pitzer F, Dantes A, Fuchs T, Baumeister W and Amsterdam A. (1996). *FEBS Letters,* **394,** 47 – 50.
Qadri I, Maguire H and Siddiqui A. (1995). *Proc. Natl. Acad. Sci. USA,* **92,** 1003 – 1007.
Renner M, Haniel A, Burgelt E, Hofschneider PH and Koch W. (1995). *J. Hepatol.,* **23,** 53 – 65.
Rice NR, MacKichan ML and Israel A. (1992). *Cell,* **71,** 243 – 253.
Rock KL, Gramm C, Rothstein L, Clark K, Stein R, Dick L, Hwang D and Goldberg AL. (1994). *Cell,* **78,** 761 – 772.
Rosmorduc O, Petit MA, Pol S, Capel F, Bortolotti F, Berthelot P, Bréchot C and Kremsdorf D. (1995). *Hepatology,* **22,** 10 – 19.
Rousset R, Desbois C, Bantignies F and Jalinot P. (1996). *Nature,* **381,** 328 – 331.
Schek N, Bartenschlager R, Kuhn C and Schaller H. (1991). *Oncogene,* **6,** 1735 – 1744.
Seeger M, Ferell K, Frank R and Dubiel W. (1997). *J. Biol. Chem.,* **272,** 8145 – 8148.
Seto E, Mitchell P and Yen TSB. (1990). *Nature,* **344,** 72 – 74.
Siddiqui A, Jameel S and Mapoles J. (1987). *Proc. Natl. Acad. Sci. USA,* **84,** 2513 – 2517.
Spandau DF and Lee CH. (1988). *J. Virol.,* **62,** 427 – 434.
Su F and Schneider RJ. (1996). *J. Virol.,* **70,** 4558 – 4566.
Ten RM, Paya CV, Israel N, Le Bail O, Mattei MG, Virelizier JL, Koruilsky P and Israel A. (1992). *EMBO J.,* **11,** 195 – 203.
Trier M, Staszewski LM and Bohmann D. (1994). *Cell,* **78,** 787 – 789.
Williams J and Andrisani O. (1995). *Proc. Natl. Acad. Sci. USA,* **92,** 3819 – 3823.
Yen TSB. (1996). *J. Biomed. Sci.,* **3,** 20 – 30.
Zoulim F, Saputelli J and Seeger C. (1994). *J. Virol.,* **68,** 2026 – 2030.